Electronic Supplementary Information

Tuning surface redox chemistry through trace Ni doping in Cobalt Pyrophosphate($Co_2P_2O_7$) for high-performance supercapacitors: Experimental and theoretical insights

Kismat K Sahoo,[a, #] Abhisek Padhy,[a, #] Ashutosh Sahoo [a] and J. N. Behera [a*]

[a]*School of Chemical Sciences, National Institute of Science Education and Research (NISER), An OCC of Homi Bhabha National Institute (HBNI), Khordha, Bhubaneswar 752050, Odisha, India.*

[b]*Centre for Interdisciplinary Sciences (CIS), NISER, Jatni, Khurda, Bhubaneswar 752050, Odisha, India.*

*Email: jnbehera@niser.ac.in

1 Electrochemical measurement: (SP300 workstation)

Electrochemical measurements were conducted in a three-electrode configuration with 3M KOH as the electrolyte. A Hg/HgO (3M KOH) electrode served as the reference, while a Pt wire acted as the counter electrode. The working electrode was prepared via the drop-casting method: 8 mg of the as-prepared GC@$Co_{0.9}Ni_{0.1}P_2O_7$ sample was mixed with 1 mg of PVDF (as a polymeric binder) and 1 mg of carbon black. The mixture was thoroughly ground using a mortar and pestle with 200 μL of ethanol and dried at room temperature. This procedure was repeated three times to ensure a homogeneous blend.
Subsequently, 2 mg of the resulting mixture was dispersed in 35 μL of DMF in an Eppendorf vial and subjected to ultrasonication for 15 minutes. The dispersed solution was then used as an ink, and was drop-casted onto a graphite sheet with an active area of 1 × 1 cm^2, yielding a total catalyst loading of 1.5 mg.
For electrochemical measurements, cyclic voltammetry (CV) was performed within a potential window of 0 to 0.5 V vs. Hg/HgO, running at various scan rates. Galvanostatic charge-discharge (GCD) measurements were carried out at current densities ranging from 1.5 to 10 A g^{-1}. Additionally, electrochemical impedance spectroscopy (EIS) was performed using an AC voltage with a frequency range of 200 kHz to 0.01 Hz at open circuit potential (OCP, E = 0.0 V).

The specific Capacitance (C_{sp}) (Fg-1) was measured from both CV and GCD techniques.

From CV curve by using the following mathematical formula (Equation 1)

$$C_{sp} = \frac{\int I(V)\, dV}{2m\, \Delta V \left(\frac{dV}{dt}\right)} \ldots\ldots\ldots\ldots (1)$$

Where, $\int I\,(V)\, dV$ denotes integrated CV area, (dV/dt) as CV scan rate (mVs^{-1}), I is associated to the discharge current (A), m is the total mass of as prepared ink loaded in the working electrode (mg), & ΔV, designates operational voltage window (V).

Further, the C_{sp} calculated by GCD techniques with the mathematical formula Shown below (Equations 2)

$$C_{sp} = \frac{I\Delta t}{m\Delta V} \ldots\ldots\ldots\ldots (2)$$

I denote the current (A) used to perform the GCD test.

2. Hybrid Device Construction:

A hybrid device was constructed using two electrodes set up. Herein, rGO (AC) and electrochemically activated $Ni_{60}Co_{40}$ 600 material are considered as negative and positive electrodes respectively. The final mass loading of the electrodes was optimized by the charge mass balance equation following (Equation 5)

$$m_+/m_- = C_+ V_+ / C_- V_- \quad \text{----------(3)}$$

Where, m_+, m_- are the mass loading, C_+, C_- are specific capacitance (F g^{-1}) & V_+, V_- are the individual operational voltage window of the positive and negative electrodes, respectively.

The energy density (E) & Power density (P) of the hybrid device were measured by following the mathematical formula (Eq. 4 & 5 respectively)

$$E = \frac{C_{sp}\Delta V^2}{2}\frac{1000}{3600} \ldots\ldots\ldots\ldots\ldots\ldots\ldots\ldots\ldots\ldots (4)$$

$$P = \frac{E}{\Delta t}\ 3600 \ldots\ldots\ldots\ldots\ldots\ldots\ldots\ldots\ldots\ldots\ldots (5)$$

Where Csp denotes specific capacitance (Fg^{-1}), ΔV is the operational voltage window, and Δt is the discharge time of the pseudocapacitor. E, P indicate energy density ($Whkg^{-1}$) and power density (Wkg^{-1}), respectively.

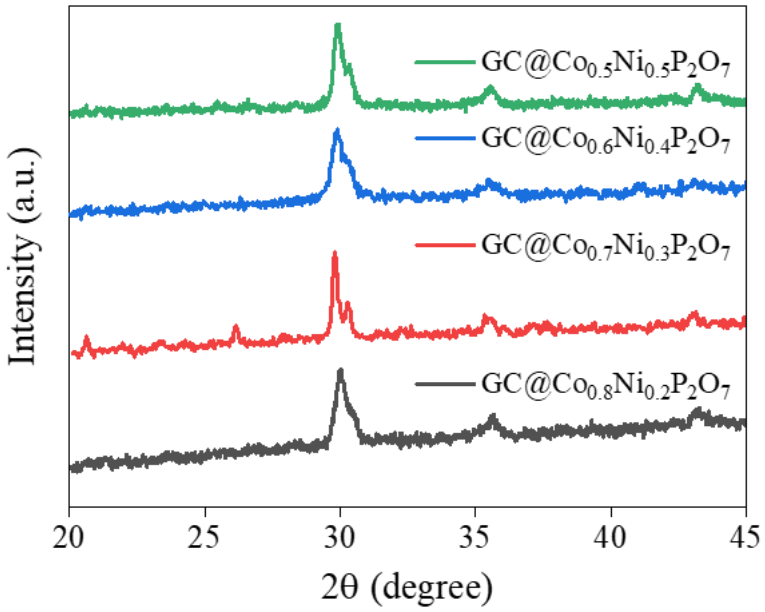

Figure S1. PXRD of other pyrophosphate variants

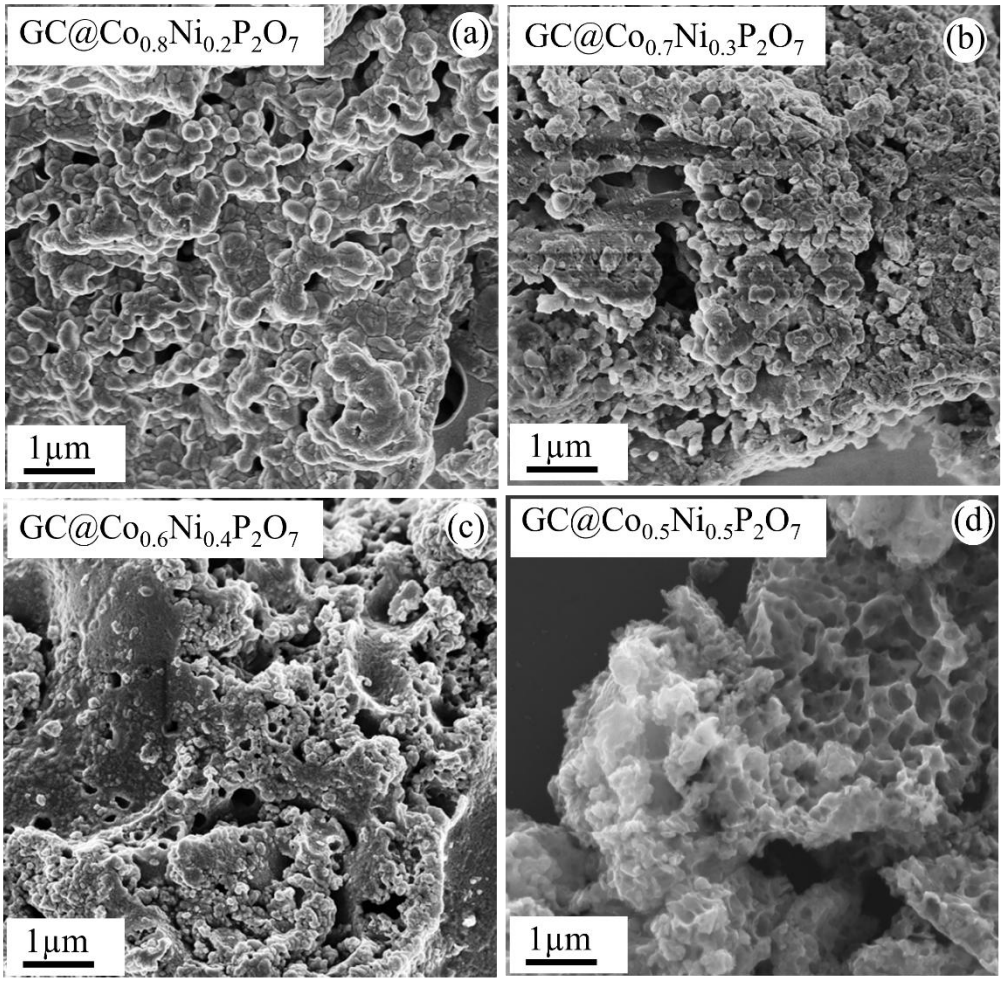

Figure S2. FE-SEM images of (a) $GC@Co_{0.8}Ni_{0.2}P_2O_7$, (b) $GC@Co_{0.7}Ni_{0.3}P_2O_7$, (c) $GC@Co_{0.6}Ni_{0.4}P_2O_7$, (d) $GC@Co_{0.5}Ni_{0.5}P_2O_7$

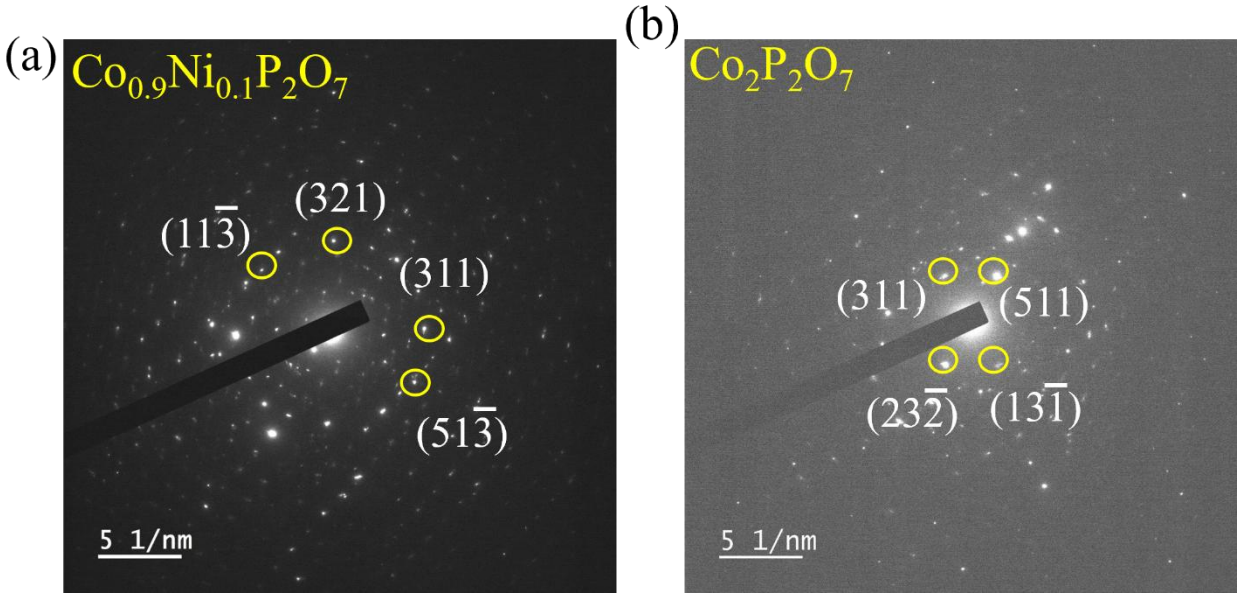

Figure S3 SAED pattern of (a) GC@$Co_{0.9}Ni_{0.1}P_2O_7$, (b) GC@$Co_2P_2O_7$

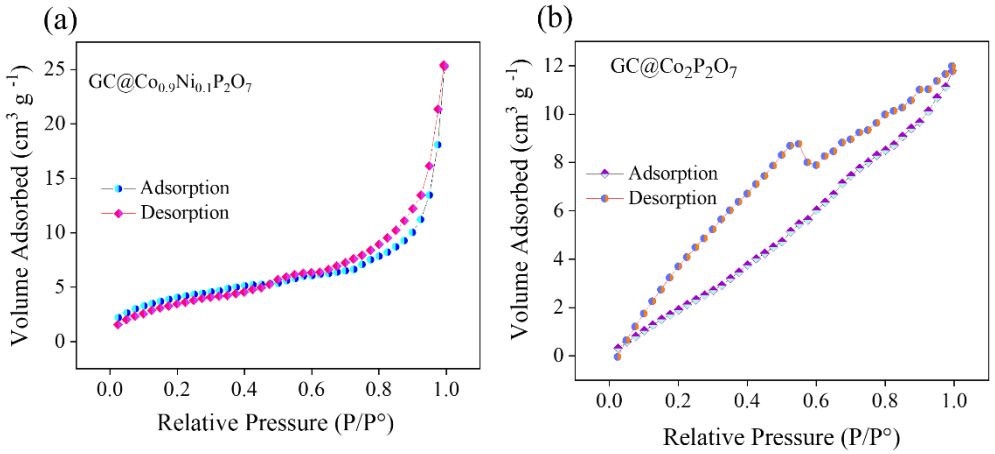

Figure S4. Adsorption/desorption isotherm for (a) GC@$Co_{0.9}Ni_{0.1}P_2O_7$, (b) GC@$Co_2P_2O_7$

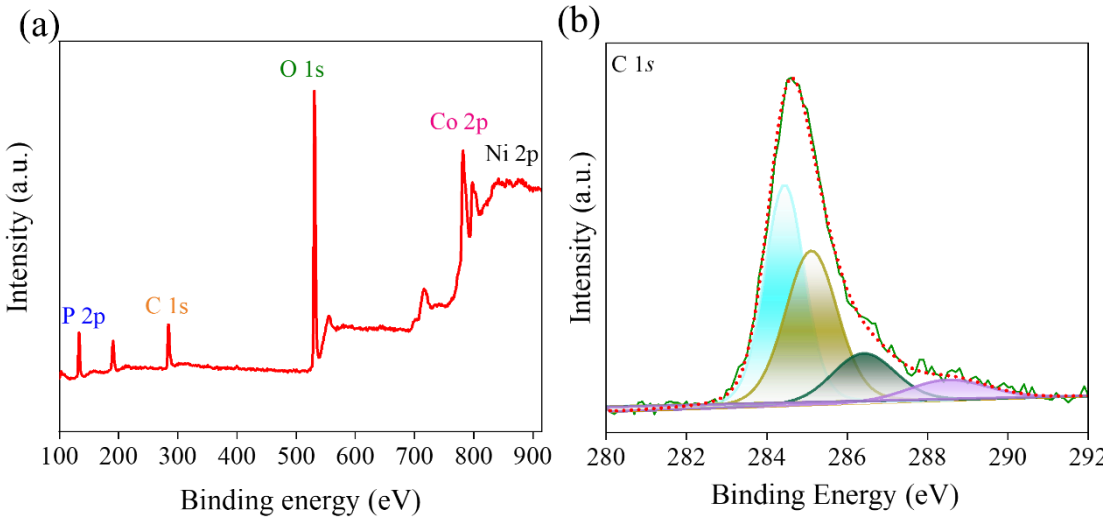

Figure S5. (a) Full survey spectrum of GC@$Co_{0.9}Ni_{0.1}P_2O_7$ and (b) deconvolution of C1s

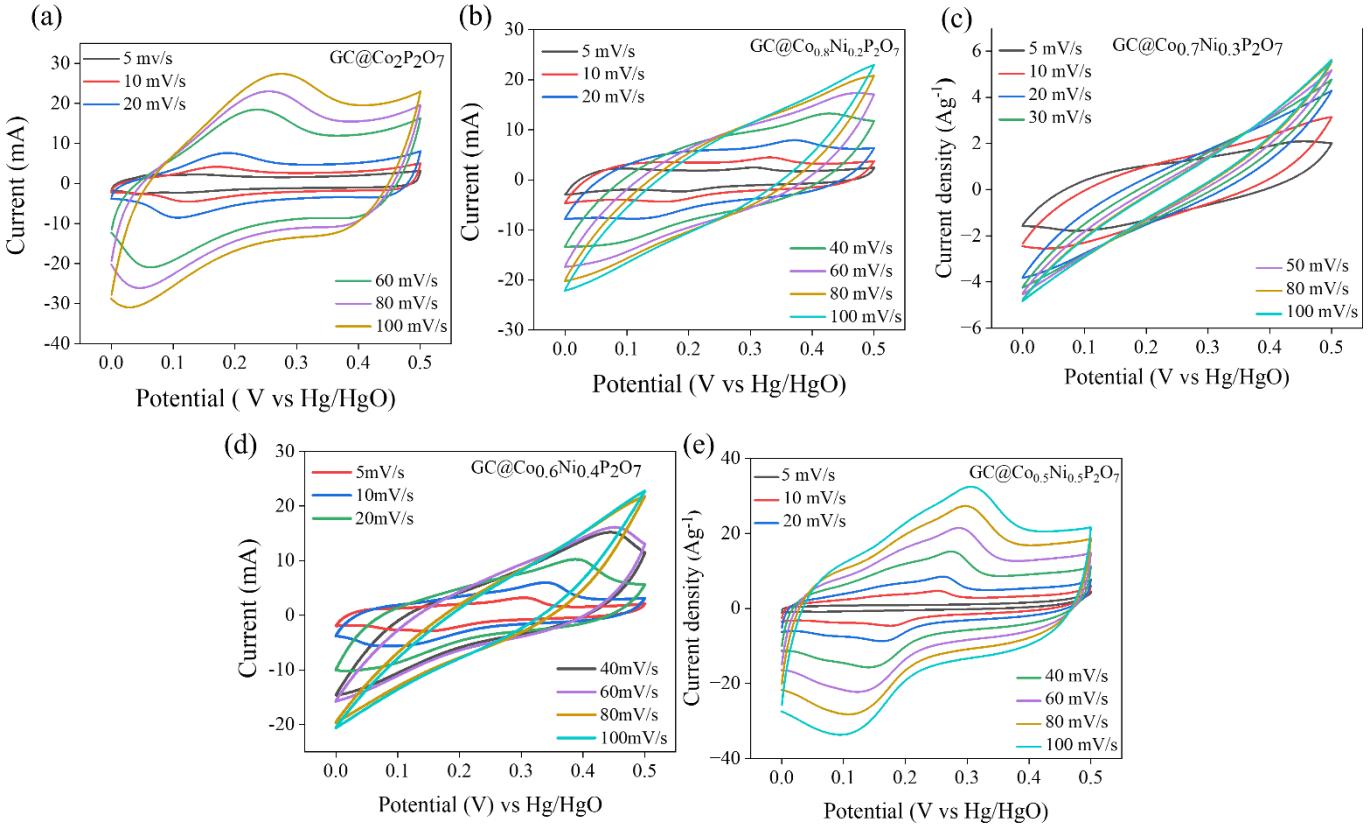

Figure S6. Cyclic voltammograms of (a) GC@$Co_2P_2O_7$, (b) GC@$Co_{0.8}Ni_{0.2}P_2O_7$, (c) GC@$Co_{0.7}Ni_{0.3}P_2O_7$, (d) GC@$Co_{0.6}Ni_{0.4}P_2O_7$, (e) GC@$Co_{0.5}Ni_{0.5}P_2O_7$

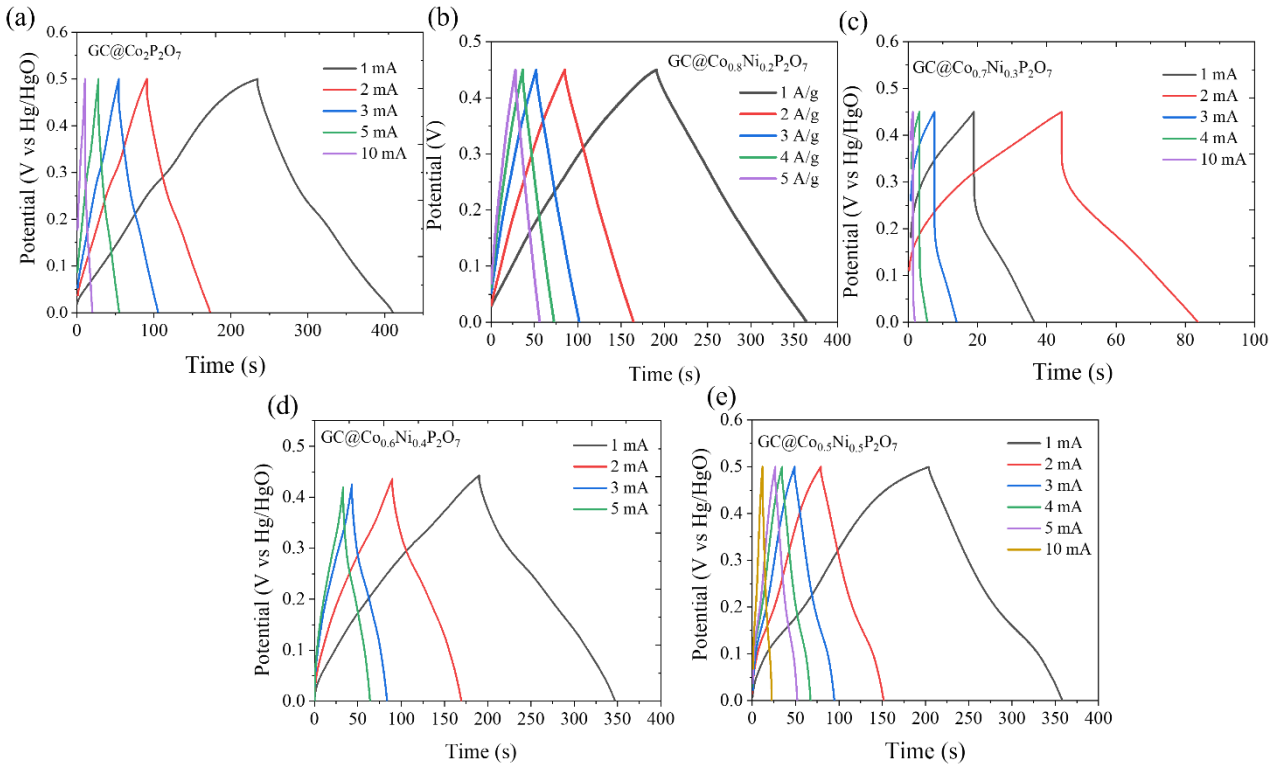

Figure S7 GCD profiles of remaining variants

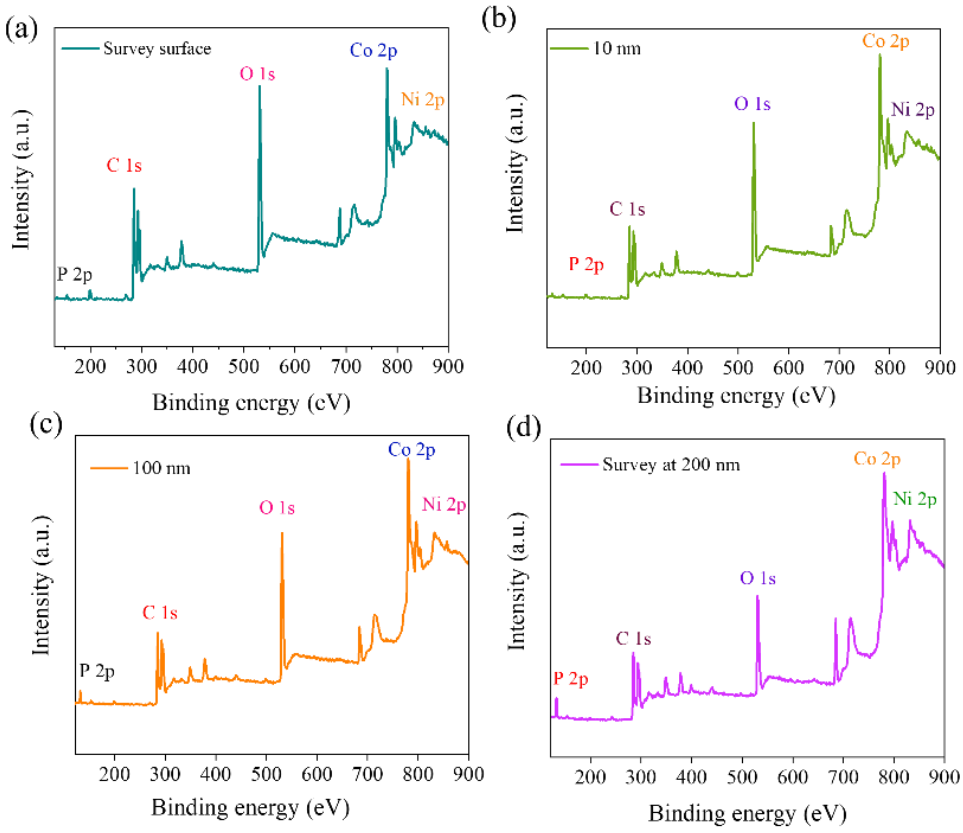

Figure S8 Survey of GC@$Co_{0.9}Ni_{0.1}P_2O_7$ at different depths.

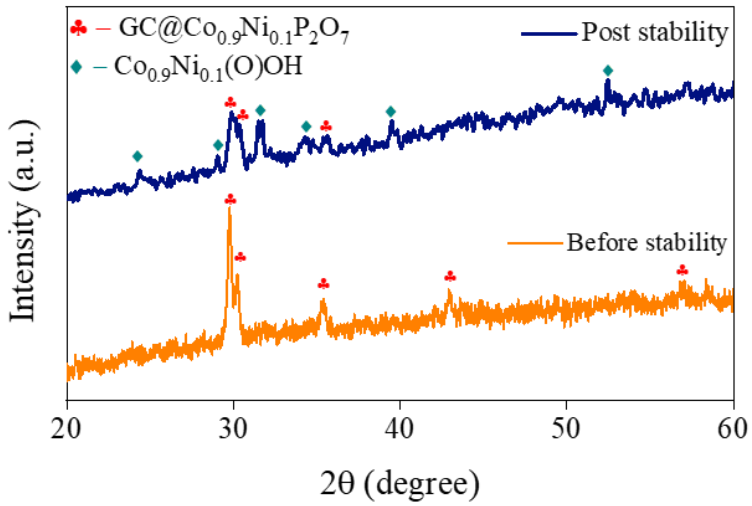

Figure S9 PXRD of before and post stability for GC@$Co_{0.9}Ni_{0.1}P_2O_7$

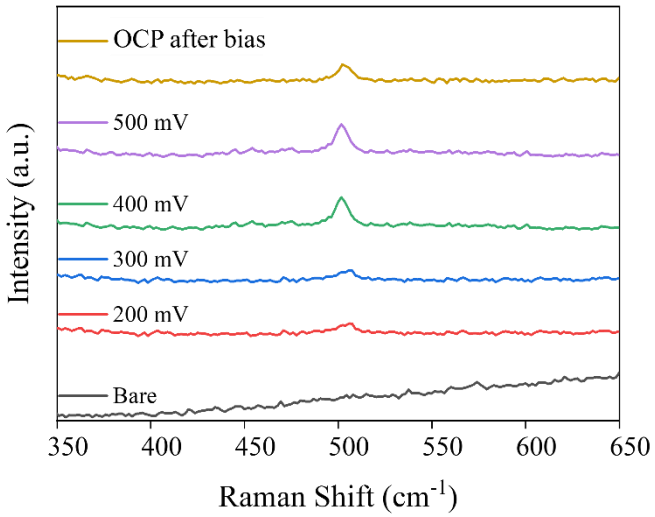

Figure S10. In-situ RAMAN study of as synthesized GC@$Co_{0.9}Ni_{0.1}P_2O_7$

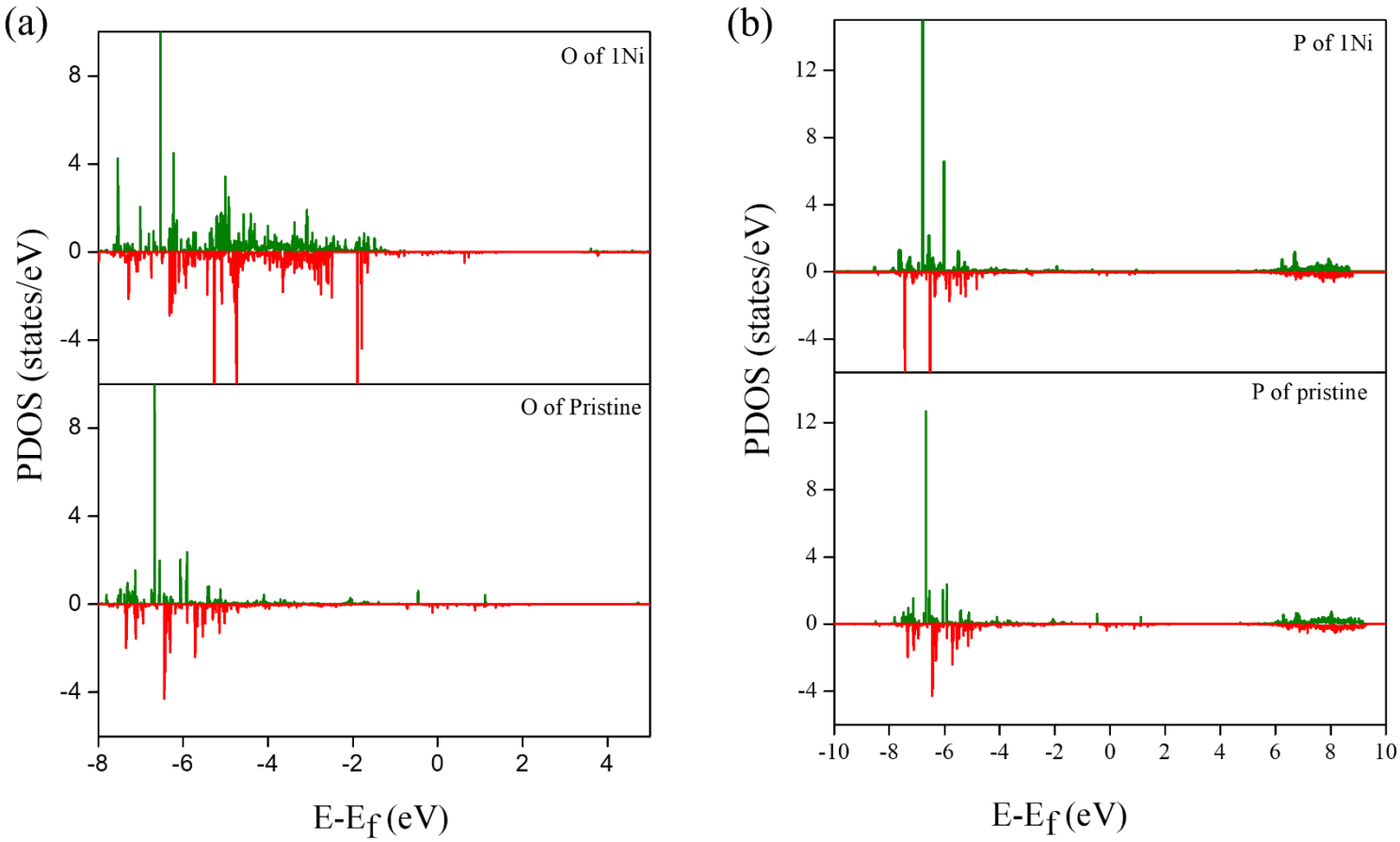

Figure S11 PDOS analysis of O (a) and P (b) in both pristine and 1Ni $Co_2P_2O_7$

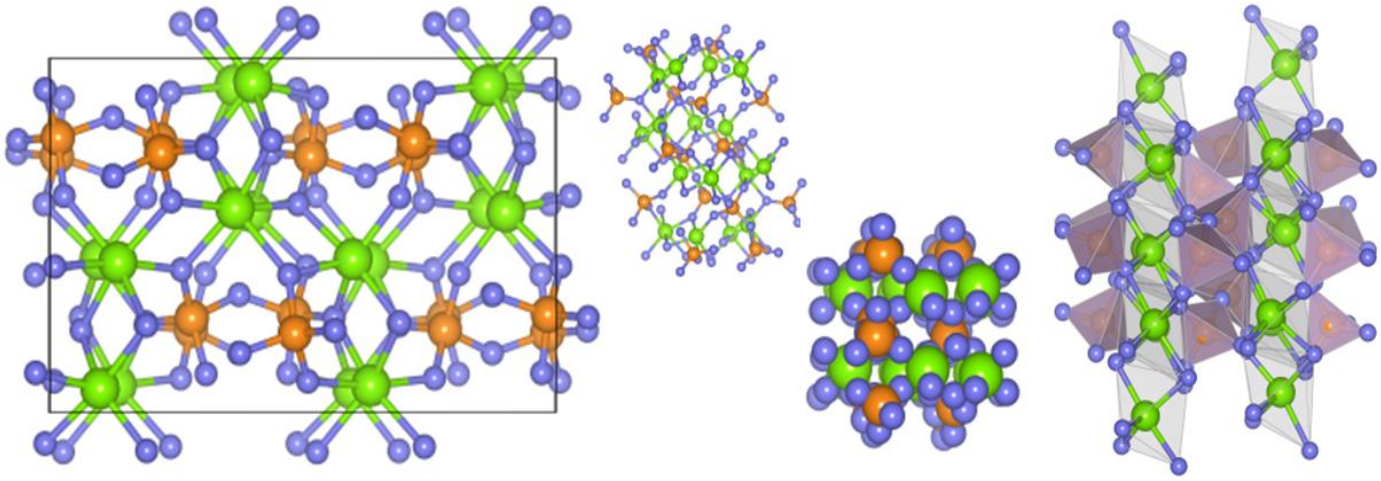

Figure S12 Different viewsof bulk Co2P2O7 where green color refers to Co orange refers to Phosphorous and purple shows Oxygen

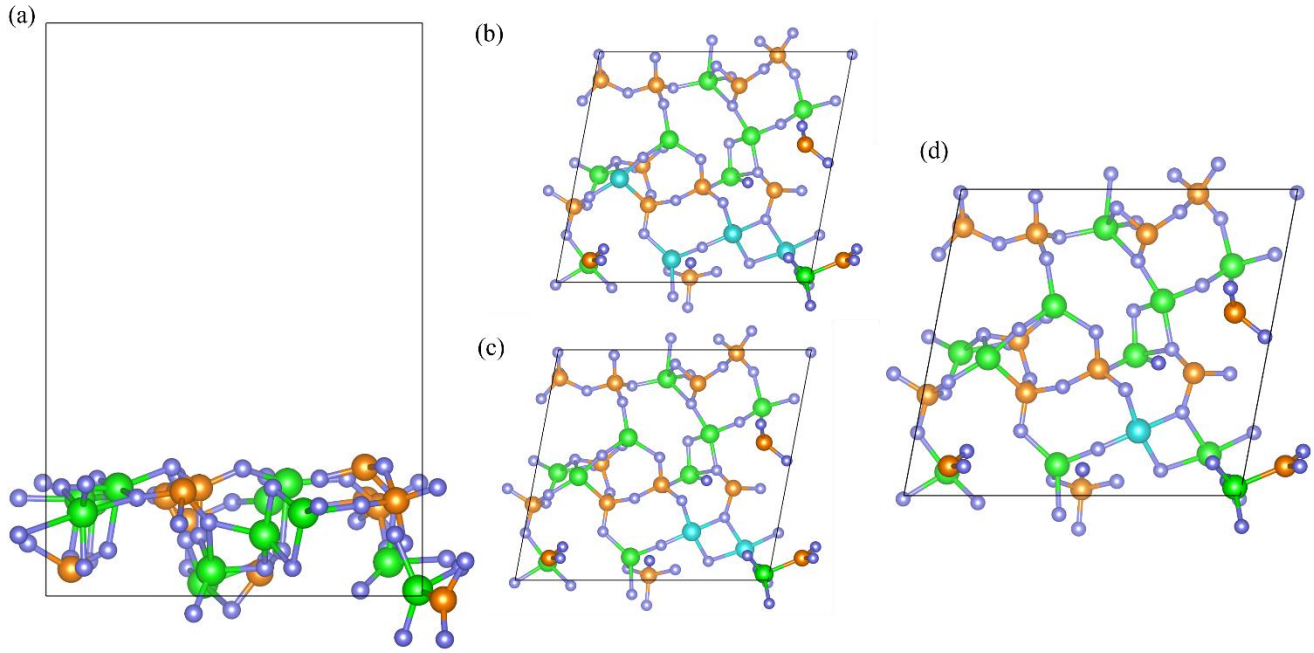

Figure S13 022 surface of different specie where a is for Pristine (b) 2Ni, (c) 4Ni and (d) refers to 1Ni here green color refers to Co, orange refers to Phosphorous, purple shows Oxygen and cyan

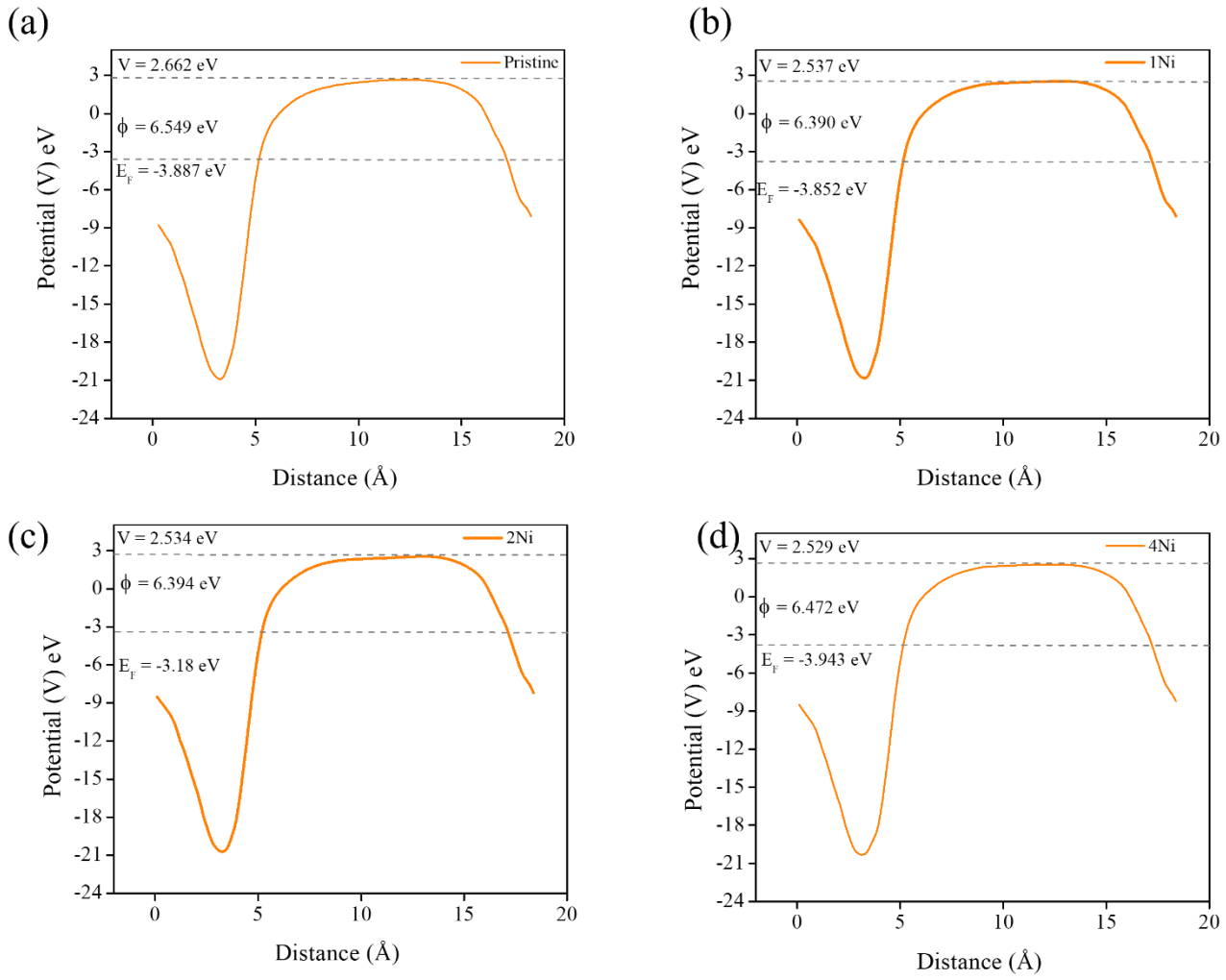

Figure S14 work function plots for each specie, such as (a) for pristine, (b) for 1Ni, (c) for 2Ni (d) for 4Ni

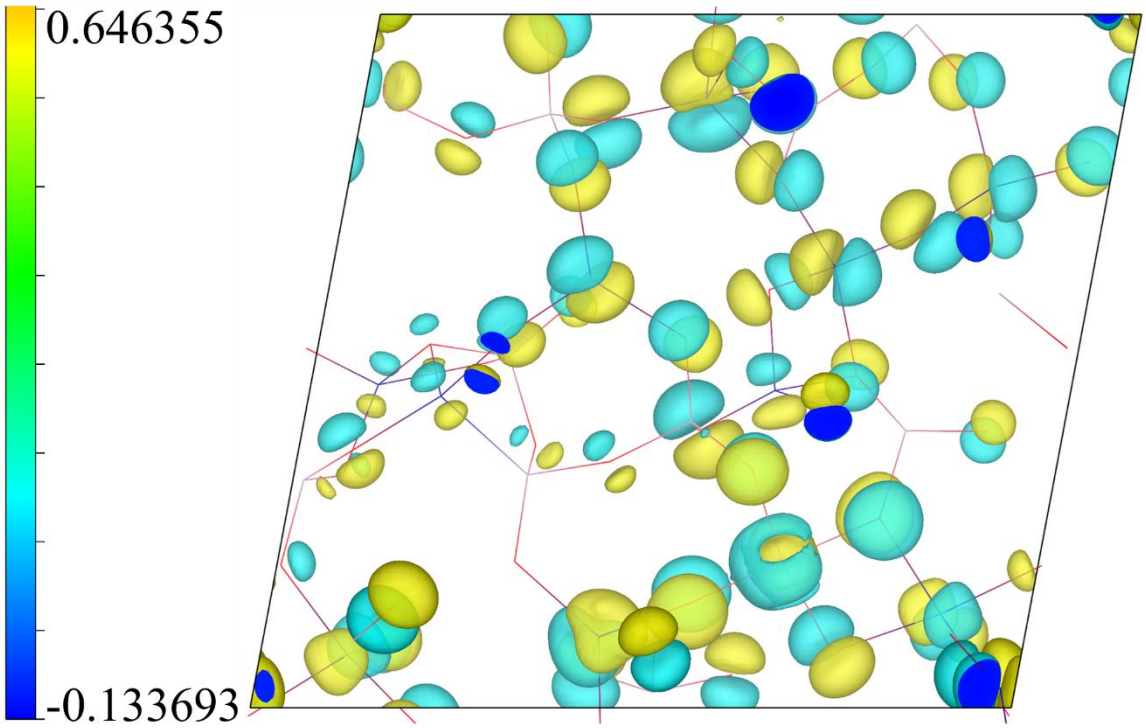

Figure S15. Charge density difference (CDD) plot produced by subtracting pristine from 1 Ni doped Co2P2O7 where blue is negligible electron

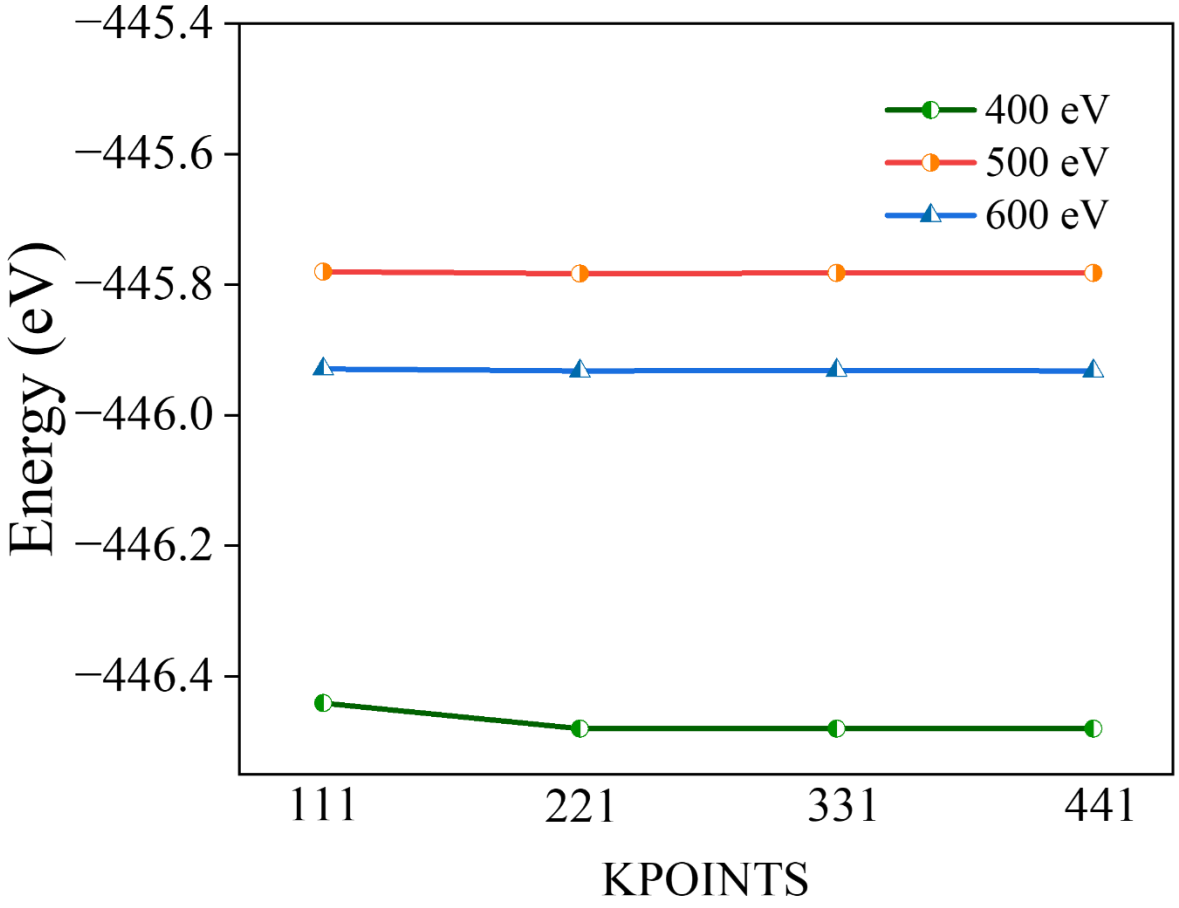

Figure S16. KPOINTS and ENCUT convergence test

Table S1 Bader analysis of the material before and after incorporation of 1Ni

Sample	Average e^- on Co	Average e^- on P	Average e^- on O	Observation
Pristine $Co_2P_2O_7$	7.59	0.685	7.634	Baseline charge distribution without dopant influence.
1Ni $Co_2P_2O_7$	7.58	0.688	7.658	Slight decrease in Co charge implies higher oxidation; electron accumulation on P and O centres indicates Co–O bond polarization.

Table S2: Summary of XPS fitting constraints used for GC@$Co_{0.9}Ni_{0.1}P_2O_7$

Parameter	Co 2p	Ni 2p	P2p	O1s
Software	CasaXPS	CasaXPS	CasaXPS	CasaXPS
Background	Shirley	Shirley	Shirley	Shirley
Peak shape	Gaussian–Lorentzian (GL)	Gaussian–Lorentzian (GL)	Gaussian–Lorentzian (GL)	Gaussian–Lorentzian (GL)
Spin orbit splitting	~15.0–15.9 eV ($2p_{3/2}$–$2p_{1/2}$)	~17.2–17.8 eV ($2p_{3/2}$–$2p_{1/2}$)	~0.84–0.88 eV ($2p_{3/2}$–$2p_{1/2}$)	----------
Area ratio 2p3/2 :2p1/2	Fixed at 2:1	Fixed at 2:1	Fixed at 2:1	----------
FWHM constraints	Same FWHM for each doublet	Same FWHM for each doublet	Same FWHM doublet	Independent components
Satellite peaks	Included (~5–6 eV above main peak)	Included (~5–6 eV above main peak)	----------	----------
Same constraints used for pristine and cycle	yes	yes	yes	yes

Table S3: Depth-resolved XPS atomic ratios for GC@$Co_{0.9}Ni_{0.1}P_2O_7$

Sample condition	Sputtering depth	P/Co atomic ratio
Before cycling	Surface	~1:1
After cycling	Surface	~0.07
After cycling	10nm	~0.5
After cycling	100nm	~1:1
After cycling	200nm	~1:1

Table S4: Comparison table for phosphate-based material.

Name	Specific Capacitance	Potential window	Specific Capacitance of ASC	Energy density (In Wh kg^{-1})	Power density (In W kg^{-1})	Capacitance retention & Cycle No.s	Ref.
Na Doped $Ni_2P_2O_7$	557 Fg^{-1} (at 1.2 A g^{-1})	0 – 0.42 V	32.6 $mFcm^{-2}$ (at 0.5 mA cm^{-2})	23.4	1292.2	97.3% retention after 1000 cycles	**1**
Amorphous $Co_{0.2}Ni_{0.8}$ polyphosphate	1259 F/g at 1.5 A/g (3M KOH)	0 – 0.55 V	119 F/g at 1 A/g	42.4	800	80% retention after 2000 cycles (Device)	**2**
$Ni_3P_2O_8$ - $Co_3P_2O_8.8H_2O$	1974 F/g at 0.5 A/g (6M KOH)	0 – 0.4 V	94 F/g at 0.5 A/g	33.4	399	83% retention after 5000 cycles (Device)	**3**
$Co_{0.4}Ni_{1.6}P_2O_7$/Ndoped graphene (NG) composites	1473 F/g at 1 A/g (3M KOH)	0 – 0.55 V	-	34.9	800	70% retention after 5000 cycles (device)	**4**
sodium doped $Ni_2P_2O_7$-$Co_2P_2O_7$	295.2 Cg^{-1} at 2 A/g (3 M KOH)	0 – 0.45 V	-	54.1	1700	95% retention after 2000 cycles (device)	**5**
$Ni_{60}Co_{40}$ 600	566 Fg^{-1} (at 1Ag^{-1})	0 – 0.65V	42 F g^{-1}	18.79	15 965.2	94% (up to 5000 cycles) & 84% (up to 10000 cycles)	**6**
$Ni_2P_2O_7$ (CTAB)	250 Fg^{-1} (at 2 Ag^{-1})	-0.1– 0.55V	70 F g^{-1}	23	775	70% (4500 cycles) (device)	**7**
$Co_2P_2O_7$ with redox additive $K_3Fe(CN)_6$	580Fg^{-1} (at 1Ag^{-1})	-0.2– 0.48V	-	-	-	96% (5000 cycles)	**8**
Nickel doped carbon/cabalt pyrophosphate hybrid	490.196 F/g at 1.5 A/g (3 M KOH)	0 – 0.5 V	55.55 F/g at 1 A/g	26.23	1859.22	80% retention after 10,000 cycles (device)	This work

References:

1. M. Haghani and S. Daneshpazhuh, *J. Environ. Anal. Chem.*, **2020**, *7*, 273.

2. L. Hou, L. Lian, D. Li, J. Lin, G. Pan, L. Zhang, X. Zhang, Q. Zhang and C. Yuan, *RSC Adv.*, **2013**, *3*, 21558–21562.

3. C. Chen, N. Zhang, Y. He, B. Liang, R. Ma and X. Liu, *ACS Appl. Mater. Interfaces*, **2016**, *8*, 23114–23121.

4. M. Pramanik, R. R. Salunkhe, M. Imura and Y. Yamauchi, *ACS Appl. Mater. Interfaces*, **2016**, *8*, 9790–9797.

5. P. Sun, Z. Li, L. Zhang, C. Dong, Z. Li, H. Yao, J. Wang and G. Li, *J. Alloys Compd.*, **2018**, *750*, 607–616.

6. A. Roy, H. R. Inta, S. Ghosh, H. V. S. R. M. Koppisetti, A. Mondal, B. R. Verma, S. Bag and V. Mahalingam, *J. Mater. Chem. A*, **2024**, *12*, 4086–4098.

7. M. Priyadharshini, M. Sandhiya, M. Sathish, T. Pazhanivel, G. Mani, A. A. Alothman and K. N. Alqahtani, *J. Mater. Sci.: Mater. Electron.*, **2022**, *33*, 9269–9276.

8. Z. Khan, B. Senthilkumar, S. Lim, R. Shanker, Y. Kim and H. Ko, *Adv. Mater. Interfaces*, **2017**, *4*, 1700059.